

Dynamic properties of multiple grating formation in doped and thermally treated lead germanate

S. Mendricks, X. Yue, R. Pankrath, H. Hesse, D. Kip

Fachbereich Physik, Universität Osnabrück, D-49069 Osnabrück, Germany
 (Fax: +49-541/969-2670, E-mail: smendric@physik.uni-osnabrueck.de)

Received: 18 November 1998/Published online: 7 April 1999

Abstract. During holographic recording in lead germanate ($\text{Pb}_5\text{Ge}_3\text{O}_{11}$) crystals two types of refractive-index gratings are observed. One has a very fast response whereas the second builds up comparably slowly. Measurements of diffraction efficiency and two-beam coupling are carried out to study the formation of both gratings and to obtain the relative phase between them. Differently doped and thermally treated samples are divided into four classes due to their different time evolution of diffraction efficiency and of the energy transfer direction during two-beam coupling. The classification depends on doping and treatment. For Ni-doped and thermally treated samples dark and photo conductivities corresponding to the slow grating are determined, indicating that Ni-doping combined with oxidation enhances the properties of the slow grating.

PACS: 42.70.Nq; 42.65.Hw

In many oxide crystals inhomogeneous illumination leads to an excitation and redistribution of charge carriers. A space-charge field builds up, which modulates the refractive index via the electrooptic effect. This so-called photorefractive effect can be used for optical data storage and signal processing [1]. Besides the search for new photorefractive materials, the tailoring of the properties of these materials gained much attention in recent years.

Lead germanate ($\text{Pb}_5\text{Ge}_3\text{O}_{11}$) is ferroelectric below $T_C = 178^\circ\text{C}$ and belongs to the point group 3. The linear electrooptic coefficients r_{13} and r_{33} are considerably large with values of 10.5 and 15.3 pm/V, respectively [2]. Krolikowski et al. [3] demonstrated that a nominally pure $\text{Pb}_5\text{Ge}_3\text{O}_{11}$ sample exhibits photorefractive effects. In previous reports [4, 5] we presented basic parameters for nominally pure and for doped crystals, as well as for $(\text{Pb}_{1-x}\text{Ba}_x)_5\text{Ge}_3\text{O}_{11}$ solid solutions. Additionally, the influences of pyroelectric fields on the dynamics of diffraction efficiency were discussed [6].

During holographic recording two kinds of refractive-index gratings are observed: A fast one with time constants generally less than 1s, and a slow one which reaches a saturated diffraction efficiency within the range from minutes to hours. Whereas a fast grating response is generally required for signal processing or interferometric applications, a slow grating is applicable in holographic data storage. Due to the fact that in lead germanate these two types of gratings are observed, it is of interest to investigate the dynamic behavior of the gratings in detail. The parameters which are presented in [4–6] are mainly related to the fast grating. Preliminary results on the slow grating were reported under the condition of small writing beam intensities ($I < 1 \text{ W/cm}^2$) [7]. In this report we focus on a general overview of the formation of both gratings. Furthermore, in Ni-doped lead germanate dark and photo conductivities related to the slow grating are systematically studied depending on dopant concentration and thermal treatment.

1 Crystal growth and sample preparation

In 1959 Speranskaya et al. [8] reported about the composition $\text{Pb}_5\text{Ge}_3\text{O}_{11}$ in the system PbO-GeO_2 for the first time. Large single-crystals were first grown in 1971 by Iwasaki et al. [9]. Lead germanate melts congruently at 738°C . Our crystals were grown at the Crystal Growth Laboratory of the University of Osnabrück using the Czochralski technique. Doping is performed by adding oxides of the dopant material to the melt. In the case of $(\text{Pb}_{1-x}\text{Ba}_x)_5\text{Ge}_3\text{O}_{11}$ solid solutions, the composition $\text{Ba}_5\text{Ge}_3\text{O}_{11}$ is prepared by the reaction of $5 \times \text{Ba}(\text{NO}_3)_2$ and $3 \times \text{GeO}_2$ at 1100°C for 3 h. This composition is added to the melt in different concentrations. After cutting and polishing to optical quality, samples were poled to the single-domain state by heating up to a temperature above T_C . During the cooling down to room temperature we applied an electric field of about 0.3 kV/cm. Samples were thermally treated either for oxidation at 600°C in O_2 (5 h) or for reduction at 350°C in 20% $\text{H}_2/80\% \text{ N}_2$ (1 h). In Table 1 we summarize the investigated samples of this work.

Dedicated to Prof. Dr. Eckard Krätzig on the occasion of his 60th birthday.

Table 1. Description of the samples used in the experiments. The samples are named as follows: (Dopant) (Mol-ppm) (Treatment). The treatments are: ag (as-grown), red (reduced) and ox (oxidized). The notation Ba20000ag represents an as-grown $(\text{Pb}_{0.98}\text{Ba}_{0.02})_5\text{Ge}_3\text{O}_{11}$ sample)

Sample	width	thickness	c axis /mm ³
Pure ag	6.20	2.40	5.50
Pure red	5.75	2.40	5.12
Pure ox	3.25	2.35	3.70
Ba20000ag	4.10	2.60	4.40
Rh500ag	4.65	2.50	6.85
Yb50ag	4.75	2.95	7.45
Yb50red	3.15	2.25	3.80
Yb50ox	3.30	2.30	4.15
Ni100ag	4.15	1.10	5.10
Ni650ag	4.00	2.40	4.25
Ni1000ag	3.15	1.85	4.80
Ni1000red	3.10	1.90	4.10
Ni1000ox	3.15	1.85	4.35
Ni2000ag	4.02	2.36	3.75
Ni2000red	4.25	2.40	4.00
Ni2000ox	4.85	2.65	5.90

2 Experimental methods

A holographic setup is used to measure the dynamic properties of the gratings in doped and thermally treated lead germanate crystals: two expanded extraordinarily polarized beams of an Ar⁺ laser ($\lambda = 488$ nm) with the same intensity ($I_1 = I_2 = 4$ W/cm²) are utilized to write gratings with a grating spacing of 1.2 μm and with the grating vector parallel to the c axis of the sample. The time evolution of the diffraction efficiency is monitored by a weak extraordinarily polarized He-Ne laser beam ($\lambda = 633$ nm, $I = 0.3$ W/cm²) which is incident at the Bragg angle. Behind the crystal the intensities of both writing beams and of the transmitted and diffracted red beams are detected by photodiodes and recorded with a storage oscilloscope.

2.1 Time evolution of diffraction efficiency

Measurements of the evolution of diffracted intensity in time are carried out for all samples. The recording and erasure cycle consists of four steps: at first the sample is preilluminated for 200 s with one of the writing beams ($\lambda = 488$ nm, $I = 4$ W/cm²). Large transient influences of pyroelectric fields on the recording behavior can be suppressed in this way [6]. In the second step the gratings are recorded for 600 s ($\lambda = 488$ nm, $I = 8$ W/cm²). The third step includes the stopping of recording and the full decay of the fast grating. Then only the slow grating remains and decays in the dark. From the time constant of this decay the dark conductivity corresponding to the slow grating is obtained. In case the slow grating is not formed within 600 s, the recording time is prolonged to check if a slow grating is formed at all. The last step of the cycle is the optical erasure of the slow grating with one of the writing beams. From the time constant of this decay the photo conductivity related to the slow grating is determined. To obtain informations about the phase relation between the two gratings, further experiments, i.e., two-beam coupling measurements, must be carried out.

2.2 Time evolution of energy transfer during two-beam coupling

From two-beam coupling experiments the energy transfer direction is obtained. This direction depends on the c axis orientation, the sign of the effective linear electrooptic coefficient (both known from previous experiments [4, 5]), and on the sign of the dominant charge carriers [10, 11]. The transmitted intensities of the writing beams behind the crystal are detected during grating recording. From the time evolution of the energy transfer direction the phase relation between the fast and the slow grating is determined. For example, a change of the energy transfer direction during the recording indicates opposite signs for the dominant charge carriers corresponding to the fast and the slow grating. In this case the gratings are 180° out of phase.

3 Experimental results

3.1 Observation of different dynamic behaviors

The general behavior of the time evolution of the fast and the slow grating can be divided into four different classes. First it is possible that only a fast grating build up. In the case of $(\text{Pb}_{1-x}\text{Ba}_x)_5\text{Ge}_3\text{O}_{11}$ solid solutions the formation of a slow grating is never observed. Even for 1 h of recording only the diffraction corresponding to the fast grating is measured (Fig. 1). For all samples the refractive-index modulation corresponding to the fast grating is in the range of 10^{-6} without external field. This measurement also demonstrates the stability of the setup for long-time recording. Crystals without slow grating are called crystals of class (a).

In most cases, a strong slow grating is formed. Its diffraction efficiency is at least comparable to or larger than that of the fast grating. The corresponding refractive-index modulations can reach values of 2×10^{-5} without an externally applied electric field. For 600 s of recording typically modulations of 10^{-6} are reached. These crystals can be divided into three further classes: (b), (c), and (d).

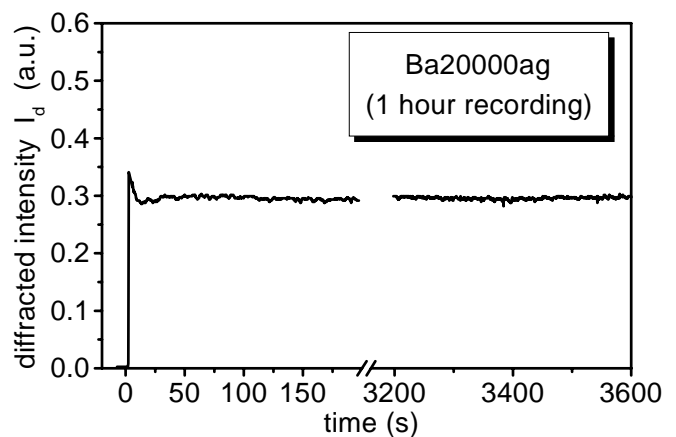


Fig. 1. Time evolution of the diffracted beam intensity I_d of the red He-Ne laser beam in a Ba20000ag (as grown $(\text{Pb}_{0.98}\text{Ba}_{0.02})_5\text{Ge}_3\text{O}_{11}$) sample. Only the fast grating is formed. Within a recording time of 1 h no slow grating appears. At the initial stage of recording the diffracted intensity is transiently enhanced due to pyroelectric fields (see [6])

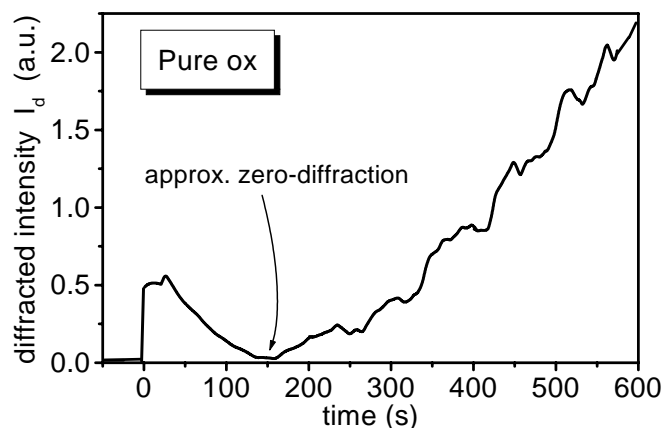


Fig. 2. Time evolution of diffracted beam intensity I_d of the He-Ne laser probe beam during 600 s of recording in a nominally pure and oxidized sample (Pure ox). The diffracted beam intensity decreases to zero within approximately 140 s and increases again to a much higher value than at the initial stage of recording

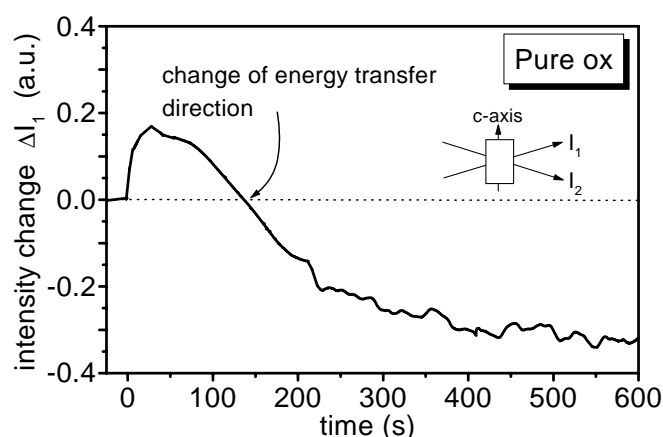


Fig. 3. Time evolution of writing beam intensity change ΔI_1 behind the crystal during recording ($I = 8 \text{ W/cm}^2$, $\Lambda = 1.2 \mu\text{m}$) for 600 s in a nominally pure and oxidized sample (Pure ox). Due to the two-beam coupling an energy transfer is observed. The energy transfer direction changes at approximately 140 s. At this time the sign of the dominant charge carriers changes from positive to negative

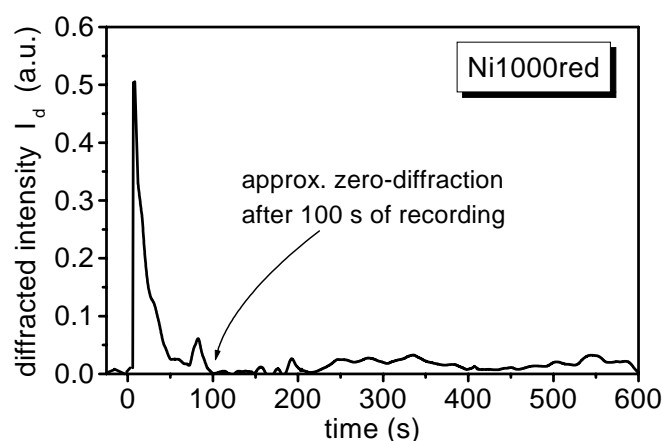


Fig. 4. Time evolution of the diffracted red beam intensity I_d during 600 s of recording ($I = 8 \text{ W/cm}^2$, $\Lambda = 1.2 \mu\text{m}$) in a Ni1000red sample. From the initial value (fast grating), the diffracted intensity I_d decreases to zero and remains zero. This indicates that the gratings are 180° out of phase and have equal amplitudes

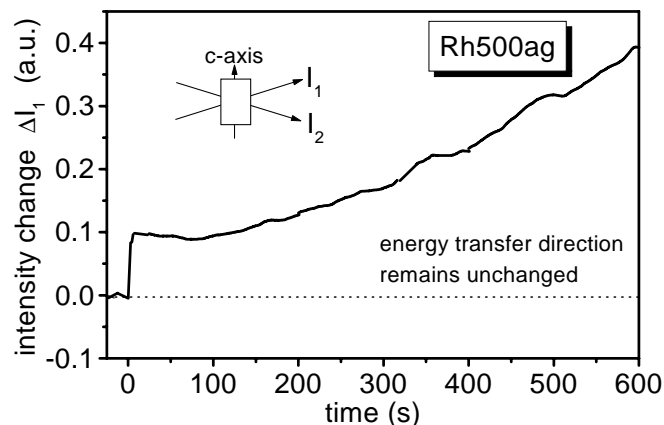


Fig. 5. Time evolution of writing beam intensity change ΔI_1 behind the crystal for the sample Rh500ag during 600 s of recording ($I = 8 \text{ W/cm}^2$, $\Lambda = 1.2 \mu\text{m}$). Due to two-beam coupling an energy transfer is observed. The intensity I_1 increases monotonously from the initial value. The energy transfer direction remains unchanged. The dominant charge carriers are positive for both gratings

In class (b) the overall diffracted intensity first decreases from the initial value to zero (compensation of the fast grating), then increases again, and reaches a sometimes much larger value than that of only the fast grating (Fig. 2). In this case, the energy transfer direction for two-beam coupling changes after the time of zero diffraction (Fig. 3), indicating that the two gratings are 180° out of phase.

In class (c) the fast grating is compensated by the slow grating and the total diffracted intensity in the steady state is zero (Fig. 4). That means the slow-grating amplitude is equal to that of the fast grating. In the two-beam coupling measurement finally no energy transfer is observed. In this case the gratings are also 180° out of phase.

The fourth class (d) includes crystals in which both gratings are in phase. After the fast grating has reached the saturated value, the diffracted intensity further increases while the slow grating builds up. The energy transfer direction remains the same, and the energy transfer between both beams increases (Fig. 5). In Fig. 6 schematic drawings of the different behaviors are given.

3.2 Classification of different lead germanate samples

From a systematic investigation we classify the investigated lead germanate samples by the four different types of behavior. This behavior depends both on doping and on thermal treatment and can be controlled in this way. In Table 2 we present the results. The $(\text{Pb}_{1-x}\text{Ba}_x)_5\text{Ge}_3\text{O}_{11}$ solid solutions are the only representatives for class (a) in which no slow grating appears. Whereas nominally pure (as-grown, oxidized, and reduced) samples always belong to class (b), in Yb- and Ni-doped samples the behavior depends on the thermal treatment. In the as-grown state these crystals belong to class (b), in the reduced state they belong to class (c), and in the oxidized state they belong to class (d). This indicates that amplitudes and phase relations (i.e., dominant charge carriers) of the gratings are influenced by thermal treatments in Yb- and Ni-doped samples. The sample Rh500ag belongs to class (d). This is the only example in which for an as-grown

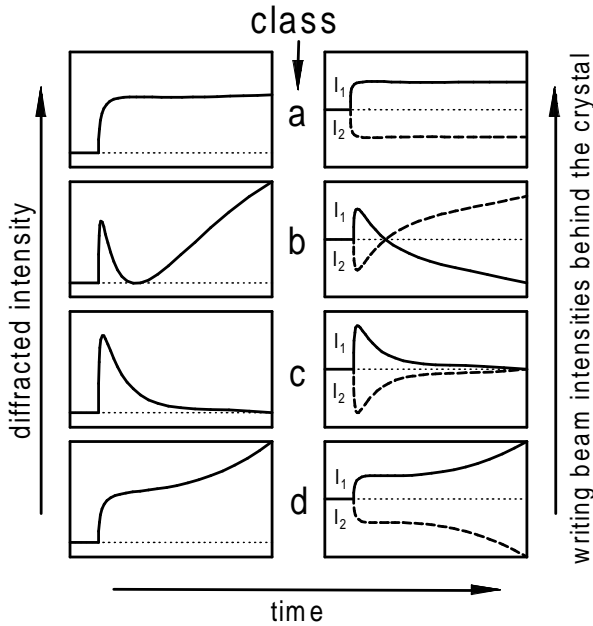


Fig. 6. Schematic drawings of the four different types of dynamic behavior for diffraction efficiency and two-beam coupling (intensities of the two writing beams (I_1 and I_2) behind the crystal). In class (a) the slow grating is not formed. In class (b) the slow grating (with larger amplitude) is 180° out of phase relative to the fast grating. Thus, the energy transfer direction changes for two-beam coupling. For crystals of class (c) the gratings are 180° out of phase and have equal amplitudes. In the steady state no diffraction or energy transfer is observed. In class (d) both gratings are in phase and the energy transfer direction remains unchanged

Table 2. Classification of the samples by their different dynamic behaviors

Class (a)	Class (b)	Class (c)	Class (d)
Ba20000ag	Pure ag Pure red Pure ox Yb50ag Ni100ag Ni650ag Ni1000ag Ni2000ag	Yb50red Ni1000red Ni2000red	Rh500ag Yb50ox Ni1000ox Ni2000ox

sample both gratings are in phase. Due to the fact that the dominant charge carriers related to the fast grating are positive for all samples [4, 5], the slow grating is formed by negative charge carriers in classes (b) and (c) and by positive charge carriers in class (d). So Rh-doping and the oxidation of Yb- and Ni-doped samples change the sign of the dominant charge carriers for the slow grating from negative to positive.

3.3 Slow grating in thermally treated Ni-doped samples

Besides the general behavior, the dark and photo conductivities corresponding to the slow grating are influenced by doping, dopant concentration, and thermal treatment. For the slow grating we determined the dark and photo conductivities in Ni-doped samples. Due to the fact that the measured conductivities are 2–3 orders of magnitude smaller than the dark and photo conductivities related to the fast grating,

Table 3. Measured values of dark and photo conductivities related to the slow grating in thermally treated pure and Ni-doped lead germanate crystals. The values are given for dark decay and optical erasure ($I = 4 \text{ W/cm}^2$) after 600 s recording with an intensity $I = 8 \text{ W/cm}^2$ and $1.2 \mu\text{m}$ grating spacing

Sample	$\sigma_{\text{dark,slow}}$ $10^{-14} (\Omega \text{ m})^{-1}$	$\sigma_{\text{photo,slow}}$ $10^{-14} (\Omega \text{ m})^{-1}$	$\sigma_{\text{photo,slow}}/\sigma_{\text{dark,slow}}$
Pure ag	0.7	6.0	8.6
Pure red	9.6	3.4	0.35
Pure ox	2.4	22.6	9.4
Ni100ag	1.5	4.5	3.0
Ni650ag	1.4	4.7	3.4
Ni1000ag	1.3	8.3	6.4
Ni1000red	14.8	13.2	0.9
Ni1000ox	0.9	28.6	31.8
Ni2000ag	1.3	12.9	9.9
Ni2000ox	0.4	27.2	68.0

we assume that the slow grating can be treated independently. The results are presented in Table 3. In as-grown Ni-doped samples the dark conductivities for four different concentrations are about the same with $\sigma_{\text{dark,slow}} = (1.3 - 1.5) \times 10^{-14} (\Omega \text{ m})^{-1}$. These values are twice as large as for the nominally pure and as grown sample (Pure ag, $\sigma_{\text{dark,slow}} = 0.7 \times 10^{-14} (\Omega \text{ m})^{-1}$). The photo conductivity of the as-grown Ni-doped samples increases with growing Ni content. After reduction (Ni1000red) the dark conductivity is increased. This behavior occurs also in the nominally pure and reduced sample (Pure red). In oxidized Ni-doped samples (Ni1000ox and Ni2000ox) the dark conductivity is decreased, while the photo conductivity is substantially increased. In the sample Ni2000ox the time constant corresponding to the slow grating dark decay is already about 25 h. For the nominally pure and as-grown sample (Pure ag) about 14 h are measured under the same conditions. However, the essential difference is the enhancement of the ratio between photo and dark conductivity. For the as-grown Ni-doped samples this ratio grows from 3.1 (Ni100ag) to 9.9 (Ni2000ag). In the sample Pure ag it is of comparable size with a value of 8.6. In the Ni-doped samples the situation changes after oxidation. Whereas in the sample Ni1000ox the ratio is 31.8, for the sample Ni2000ox we determine a value of 68.0. For the nominally pure and oxidized sample (Pure ox) with a ratio of 9.4 there is no great difference compared to the as-grown sample (Pure ag, ratio 8.6). So, regarding the slow grating, for Ni-doped and oxidized samples the photo conductivity is increased while the dark conductivity becomes even smaller.

4 Discussion

In [4] and [7] it is claimed that in lead germanate intrinsic defects may take part in the charge transport. For the fast grating we found that doping does not enhance the photorefractive effect. Nevertheless, in [5] it was described that the fast-grating response can be influenced by thermal treatments. In the case of reduction treatments the response becomes very slow for all samples. Also the dark conductivities observed in reduced samples are generally smaller. For a nominally pure and reduced sample this behavior is not observed. So in this case the doping seems to play an important role for

the dark conductivity. In [7] Yb-doped samples have shown strong dependencies of the time constants for both gratings on reduction and oxidation treatments. Furthermore, it is possible to change the sign of the dominant charge carriers for the slow-grating by oxidation. Reduction leads to a substantial increase of the time constants for the fast grating, and a significant decrease of the slow grating time constants. Again in a pure sample reduction does not lead to comparably large changes, indicating that the doping influences both gratings, especially for thermally treated samples.

4.1 Classification of different samples

From the present investigation we have the opportunity to divide the samples into different classes. We have given the results for the samples in which we clearly identified the behavior. Similar behaviors have also been reported for other materials [12–17] and can be explained theoretically [18, 19] taking into account simultaneous electron–hole transport which was first demonstrated by Orłowski and Krätzig [11].

For Yb- and Ni-doping we observe the same behavior. So Ni and Yb seem to act as photorefractive centers in a similar way. After oxidation they behave like Rh in an as-grown sample. From the present investigation it is not possible to obtain the charge states of the involved centers. The results only point to the fact that these changes of the behavior can be induced either by the doping alone (Rh), or by the combination of doping and thermal treatment (Yb, Ni).

4.2 Slow grating in thermally treated Ni-doped samples

For Ni-doped samples the dark and photo conductivities related to the slow grating are studied depending on the Ni content as well as on the thermal treatment. In [5] we presented that for the fast grating, Ni doping does not increase the photo conductivity. These measurements reveal that at least the slow grating can be enhanced systematically due to the increasing dopant concentration. A further improvement is possible after oxidation. While the dark conductivity becomes smaller the photo conductivity of the slow grating increases for oxidized Ni-doped samples. Again we can not identify the charge states of the involved Ni-centers from the present experiments.

5 Summary

Measurements of diffraction efficiency and two-beam coupling have been carried out for differently doped and thermally treated lead germanate samples indicating that doping and thermal treatments change the photorefractive properties, i.e.,

the formation and the properties of multiple gratings in lead germanate crystals. The main results can be summarized as follows:

- During holographic recording two refractive-index gratings (a fast and a slow grating) are observed.
- Differently doped and thermally treated samples are classified by four different types of the formation of both gratings.
- Doping with Ba suppresses the formation of the slow grating.
- As-grown Rh-doped and oxidized Yb- and Ni-doped samples exhibit the same behavior.
- In Ni-doped samples the properties of the slow grating are systematically studied. The photo conductivity increases with the Ni content. A further enhancement is observed after oxidation of the samples.

Still it has to be pointed out that further experiments are needed to identify the photorefractive centers and their charge states in detail to give an explanation of these results taking into account the atomistic situation.

Acknowledgements. Financial support by the Deutsche Forschungsgemeinschaft (SFB 225, A1, A6) is gratefully acknowledged.

References

1. P. Günter, J.P. Huignard (Eds.): *Photorefractive Materials and their Applications II - Topics in Applied Physics*, Vol. 62 (Springer, Berlin, Heidelberg 1989)
2. K.H. Hellwig (Ed.): *Landolt-Börnstein-Numerical Data and Functional Relationships in Science and Technology*, New Series III/16 (Springer, Berlin 1981)
3. W. Krolikowski, M. Cronin-Colomb, B.S. Chen: *Appl. Phys. Lett.* **57**, 7 (1990)
4. X. Yue, S. Mendricks, Y. Hu, H. Hesse, D. Kip: *J. Appl. Phys.* **83**, 3473 (1998)
5. S. Mendricks, X. Yue, T. Nikolajsen, R. Pankrath, H. Hesse, D. Kip: *Proc. SPIE* **3554**, 205 (1998)
6. X. Yue, S. Mendricks, T. Nikolajsen, H. Hesse, D. Kip, E. Krätzig: *J. Opt. Soc. Am. B* **16**, 389 (1999)
7. X. Yue, S. Mendricks, T. Nikolajsen, H. Hesse, D. Kip, E. Krätzig: submitted to *J. Appl. Phys.*
8. E.I. Speranskaya: *Izv. Akad. Nauk SSSR, Otdel. Khim. Nauk* **162** (1959)
9. H. Iwasaki, K. Sugii, S. Miyazama: *Mater. Res. Bull.* **6**, 503 (1971)
10. D.L. Staebler, J.J. Amodei: *J. Appl. Phys.* **43**, 1042 (1972)
11. R. Orłowski, E. Krätzig: *Solid State Commun.* **27**, 1351 (1978)
12. J.P. Herriau, J.P. Huignard: *Appl. Phys. Lett.* **49**, 1140 (1986)
13. G. Montemezzani, H. Looser, M. Ingold, P. Günter: *Ferroelectrics* **92**, 281 (1988)
14. M. Miteva, L. Nikolova: *Opt. Commun.* **67**, 192 (1988)
15. L.M. Bernardo, J.C. Lopez, O.D. Soares: *Appl. Opt.* **29**, 12 (1990)
16. M.C. Bashaw, R.C. Barker, T.-P. Ma, S. Mroczkowski, R. R. Dube: *Phys. Rev. B* **42**, 5641 (1990)
17. X. Yue, E. Krätzig, R. Rupp: *J. Opt. Soc. Am. B* **15**, 2383 (1998)
18. G.C. Valley: *J. Appl. Phys.* **59**, 3363 (1986)
19. S. Zhivkova, M. Miteva: *J. Appl. Phys.* **68**, 3099 (1990)